Structure and formation of a gel of colloidal disks

Mark Kroon, Willem L. Vos, and Gerard H. Wegdam*

Van der Waals–Zeeman Instituut, Universiteit van Amsterdam, Valckenierstraat 65, 1018 XE Amsterdam, The Netherlands

(Received 8 July 1997)

We have performed static scattering experiments on the transition in time from a fluidlike sol to a solidlike gel of a suspension of disk-shaped charged colloidal particles. The combination of static light scattering and small angle x-ray scattering probes more than three orders of magnitude in the scattering vector q. At the smallest q the static structure factor $S(q)$ shows a q^{-d} dependence in both the sol and gel state. The algebraic exponent d evolves from 2.8 to 2.1 during the gelation. We find that the sol is not comparable to a simple liquid but rather to a low-viscosity precursor of the gel. At intermediate q a plateau connects this regime to the form factor $\overline{F^2}(q)$ of the colloidal disks, which is observed at the largest q. On the plateau a small peak related to nearest-neighbor correlations is observed, which decays before gelation occurs. After application of shear on the suspensions we have observed the rapid formation of nematiclike order of the colloidal disks. This order decays in time due to reorientation of the colloidal disks while the final gel state is reached. The formation of the gel does not proceed via aggregation to form ever larger clusters. Based on our findings we propose that reorientation of the charged particles is the mechanism by which the gelation occurs. [S1063-651X(98)06702-6]

PACS number(s): 61.43.Fs, 71.55.Jv, 64.70.Pf, 82.70.Dd

I. INTRODUCTION

The spatial and orientational arrangement of particles in colloidal suspensions is determined by the interaction between the particles and by their form and symmetry. Colloidal suspensions of monodisperse spheres have a relatively simple equilibrium phase diagram determined by the volume fraction and the ionic strength, revealing gas, liquid, and solid phases [1]. Anisotropic particles, needles or disks, have their orientation as an additional degree of freedom. Since Onsager [2] we know that a system of anisotropic particles exhibits a nematic phase, which is characterized by long-range orientational order but short-range positional order. In colloidal systems of hard disks many liquid crystalline arrangements are expected. This expectation is based on a vast amount of experimental observations on molecular liquid crystals [3], on theory [2,3], and on simulations [4]. The availability of synthetic colloidal clays, made of disklike particles [5], promised the physical realization of these phases on a mesoscopic scale. These colloidal disks are charged and interact via a screened Coulomb potential with a quadrupolar symmetry.

Interestingly, suspensions of these charged colloidal disks are observed to undergo a transition from a fluidlike sol to a solidlike gel, instead of entering a liquid-crystalline phase [6–14]. This gelation process occurs as a function of time, denoted by T, at constant temperature and particle density. Recently we have performed extensive dynamic light scattering experiments on this sol-gel transition [12,13]. The measurements reveal the slowing down of the collective dynamics towards the gelation time T_g, where the sample becomes a macroscopically immobile structure without phase separation. The time of gelation can be defined rather accurately by the second moment of the scattered intensity distribution. If we consider time to be the analog of the physical control parameter, the gelation has all the characteristics of a glass transition [15], which is considered to be a dynamical transition rather than a thermodynamic one [16,17]. The colloidal disk system appears to be enduringly off-equilibrium as it evolves in time. The picture emerging is one of frustration of the particle motion by the algebraically increasing viscosity [14], barring the system from entering a crystalline state, just as in the glass transition. The essence of our experiment is that the evolution of our colloidal system is followed as a function of time at constant density and constant temperature. This is in contrast to systems where the glass transition occurs as a function of the volume fraction [18,19], temperature [20], or pressure [21].

At present, it is unknown how the structure evolves as the gelation proceeds. Generally, two different types of three dimensional ordering are proposed for the final gel state. The first one, favored by current opinion, is the ''house of cards'' structure for the gel [22,23]. This conjecture is based on the physical intuition that the short-range part of the electrostatic interaction has a strong quadrupolar character. It implies the presence of (on average) T-shaped units. This may be true for gels at high particle densities. However, the observation of the existence of strong gels at low particle densities, where the colloidal disks are more than a few diameters apart, has led to the second model, a random structure for the gel. The more isotropic long-range part of the electrostatic interaction favors this structure [6,7]. Little is known about orientational order or liquid crystalline order in this structure. Both structures are assumed to be formed by particle aggregation to form ever larger clusters [11]. Whether or not aggregation is the road to gel formation is one of the questions we will address in this paper.

In the work we present here, static light scattering (SLS) and small angle x-ray scattering (SAXS) techniques are used to investigate the time evolution of the structure and the presence or absence of liquid crystalline order. The combi-

*Electronic address: wegdam@phys.uva.nl

nation of scattering techniques probes more than three orders of magnitude in the scattering vector q. This allows us to investigate the state of the colloidal suspensions from sub-particle length scales to the large length scale colloidal arrangement. Although the starting point of the gelation is a fluidlike sol of randomly oriented individual colloidal disks, the overall shape of the static structure factor is observed to be similar to the solidlike gel. The sol can be considered a low-viscosity precursor of the solid gel. The structure factor shows algebraic behavior at small q, consistent with a fractal structure. At large q, the scattered intensity decays as q^{-2}, indicative of randomly oriented disks.

It has been shown in experiments by Willenbacher [14] that the low-viscosity initial state can be reproducingly prepared after application of shear. In our experiments the shear is applied at the moment of insertion of the sample into the cell. The system is then left to itself and the induced stresses are released by particle rearrangement. Just after the introduction into the flat-plate cell, we have observed the rapid formation of nematiclike order of the colloidal disks. The experiments show that this order is probably not the equilibrium state, because in time this order decays due to reorientation of the colloidal disks, and because the order does not appear in the many-particle correlations. The isotropic orientation is reached in the final gel state. Based on our findings we suggest that, rather than aggregation, reorientation is the mechanism behind the phenomenon of gelation in time.

This paper is organized as follows: first, we will discuss the experimental conditions in Sec. II. Then we will present the experimental results in Sec. III. We will estimate the dimensions of the colloidal disks from the form factor. We will present the static structure factor of the colloidal arrangement at different stages of the gelation. We will present the effects of shear forces applied to the colloidal suspensions, and compare this to results obtained on a dried gel. We will summarize and discuss our findings in Sec. IV.

II. EXPERIMENT

A. Sample preparation

Because of its high purity and small size, the synthetic clay laponite [5] forms colorless and transparent suspensions that are particularly suited for scattering studies. For our study we have used Laponite RD. This grade of Laponite is easy to disperse and forms strong gels at relatively low densities. The structure formula of laponite RD is $Si_8[Mg_{5.5}Li_{0.4}H_{4.0}O_{24.0}]^{-0.7}Na_{0.7}$, with a specific density $\rho = 2570$ kg/m^3. Each particle is a monocrystalline disk built up by three layers, two outer tetrahedral silicate layers and a central one consisting of octahedrally surrounded magnesia. Part of the magnesium in the central layer is replaced by lithium. In aqueous dispersions the sodium ions on the outside diffuse into the surrounding liquid and screen the negative charge of the oxygen. The result is an electrical double layer, i.e., screened Coulomb potential, surrounding the disk of which the surface charge distribution remains fixed due to the underlying crystal structure.

Laponite powder and dust-free demineralized water are slowly mixed in a certain volume fraction Φ_v, and stirred vigorously for 2 h with a magnet stirrer. After $5-10$ h the suspensions are colorless and transparent charge-stabilized

sols, where the light scattering entity is a single colloidal disk [9,12]. Here we have studied a suspension at $\Phi_v = 0.0119$, which forms a strong gel in 100 h [12] when left undisturbed, and a suspension at $\Phi_v = 0.0039$, which does not gelate within a year. With these samples we have not observed a phase separation, i.e., no sedimented dense solidified gel below a diluted gaseous suspension of colloidal discs. As time proceeds we have observed the gelating suspension to show an increased viscosity when tumbling the original stock tubes. Finally the suspension behaves as a macroscopically immobile structure, which we call the gel. The gel does not flow or adapt its shape when turned in the gravitational field. The progress of the gelation is denoted by the time T, which starts directly after mixing the components.

B. Light and x-ray scattering

In a scattering experiment the incident and scattered beams are characterized by their wave numbers $\vec{k}_i$ and $\vec{k}_s$, respectively. The momentum transfer or scattering vector q is obtained from the conservation relation $q = |\vec{q}| = |\vec{k}_s - \vec{k}_i| = 4n\pi\lambda^{-1}\sin(\vartheta/2)$, where λ is the wavelength of the incident radiation in vacuum, and ϑ the scattering angle. The refractive index n can be considered equal to unity for x rays.

The light source in the SLS setup is a He-Ne laser producing a 10 mW beam with vertical polarization at a wavelength $\lambda = 632.8$ nm. The laser beam is focused in the sample to a beam waist of 50 μm. The sample is contained in a cylindrical 10 mm diameter quartz cuvette, which is immersed in an index-matching toluene bath of 80 mm diameter. Scattered light with vertical polarization is detected by a photomultiplier that is mounted on a goniometer arm. The range in q is $9.2\times10^{-4}-2.6\times10^{-2}$ nm^{-1}. The signal to stray light ratio is better than 10^2 for all q. Speckle averaging is performed by slow (8 μm/s) vertical translation of the sample over at least 50 mm through the laser beam with a motorized setup, while measuring the scattered intensity.

Small angle x-ray scattering (SAXS) experiments were performed at the European Synchrotron Radiation Facility (ESRF) in Grenoble on the high brilliance beam line ID2/BL4 [24], and at the Daresbury Synchrotron Radiation Source (SRS) on station 8.2 [25]. At the ESRF the wavelength of the radiation is set at $\lambda = 0.0988$ nm. The range in q is $1.0\times10^{-2}-5.3\times10^{-1}$ nm^{-1}. A two-dimensional gas filled detector was employed, which allows one to study the (an)isotropy of the scattering. At the SRS the wavelength of the radiation is set at $\lambda = 0.154$ nm. The range in q is $9.9\times10^{-2}-2.3$ nm^{-1}. Here a gas filled quadrant x-ray detector was employed, which compensates for the decrease in scattering intensity towards wider scattering angles by use of larger collecting elements towards higher angles. The sample containers used here are made of a brass frame (1×4 cm^2) acting as a spacer of 0.5 mm thickness. Windows of kapton or mica are glued on both sides. The suspensions are inserted through sealable holes. We use such thin containers in the SAXS experiments due to strong x-ray absorption by water (absorption coefficient $\mu \sim 10^3$ m^{-1}). In turn, the thin plane parallel geometry of the x-ray cell was impractical to use in light scattering. The strong scattering from the window in-
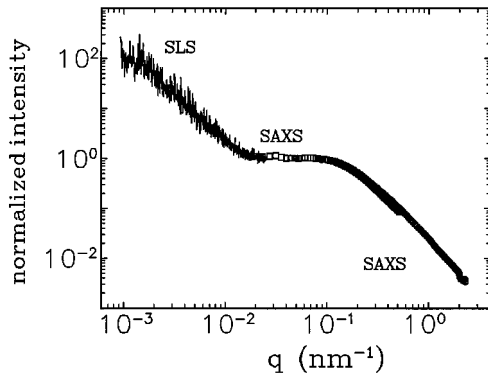
FIG. 1. Overview of the static scattered intensity $I_s(q)$ as obtained from three scattering experiments. The smallest q regime, between 10^{-3} and 10^{-2} nm^{-1}, is captured by static light scattering (SLS). The intermediate q regime, between 10^{-2} and 10^{-1} nm^{-1}, and the largest q regime, between 10^{-1} and 10^0 nm^{-1}, are captured by small angle x-ray scattering (SAXS). The intensities displayed have been scaled to merge at the regions where the range in the scattering vector q overlaps.

terfaces and the relatively low scattering from the laponite suspensions prohibited use of the same cell.

III. RESULTS

In Fig. 1 we show an overall view of the static scattered intensity $I_s(q)$ as obtained with the different scattering setups. The intensities as shown have been measured on a stable gel where no significant changes in time were observed any more. (i) At the smallest q (light), between 10^{-3} and 10^{-2} nm^{-1} a steep decrease in $I_s(q)$ is observed, which is attributed to the static structure factor $S(q)$ of the gel. (ii) There is a plateau at intermediate q values (SAXS), between 10^{-2} and 10^{-1} nm^{-1}. The corresponding length scale $2\pi/q$ is of the order of the average interparticle (center of mass) distance. (iii) At the largest q values (SAXS), between 10^{-1} and 10^0 nm^{-1}, $I_s(q)$ roughly follows a q^{-2} power-law decay, which is consistent with the form factor $F(q)$ of randomly oriented thin disks [26].

We adopt the usual assumption that the spatial arrangement of the colloidal disks is decoupled from the form factor [26]. Hence, $I_s(q)$ is separated into two factors $\overline{F^2}(q)$ and $S(q)$ by

$$I_s(q) \propto \rho I_0 S(q) \overline{F^2}(q), \tag{1}$$

where $\rho = N/V$ is the number density of individual scatterers in the sample, and I_0 is the incident intensity. The static structure factor $S(q)$ accounts for the interference of radiation scattered from the disks in the colloidal structure. The single particle form factor $\overline{F^2}(q)$ accounts for the interference of radiation scattered from different parts within the particle.

A. Form factor of colloidal disks

In order to measure the form factor $\overline{F^2}(q)$ of the colloidal disks, we have performed SAXS measurements on a dilute nongelating colloidal suspension in water, with a volume
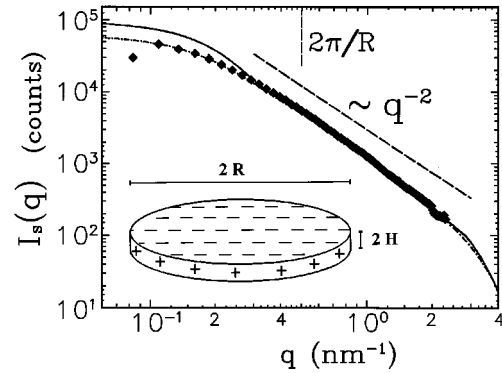

FIG. 2. Scattered intensity $I_s(q)$ (diamonds) of a dilute, nongelating, suspension of disks in the range of the form factor. At large q, the intensity decays with q^{-2} (dashed line) as expected for randomly oriented thin disks. The solid curve is the calculated form factor of monodisperse thin disks with radius $R = 12.5 \pm 0.5$ nm and a thickness $2H = 1.0 \pm 0.1$ nm. The dash-dotted curve is the calculated form factor of disks with the same dimensions with a Gaussian polydispersity in the radius of 4 nm. The colloidal disk is illustrated in the inset with its sizes and charge distribution.

fraction $\Phi_v = 0.0039$. The results are shown in Fig. 2. For a thin disk the scattered field $F(q;H,R,\phi)$ is given by [26]

$$F(q;H,R,\phi) = \frac{\sin[qH\cos(\phi)]}{qH\cos(\phi)} \times \frac{2J_1[qR\sin(\phi)]}{qR\sin(\phi)}, \tag{2}$$

where ϕ is the angle between the normal to the disk plane and the scattering vector q, $2R$ is the disk diameter, $2H$ is the thickness of the disk (see inset of Fig. 2), and J_1 is the first order Bessel function. The form factor becomes

$$\overline{F^2}(q;H,R) = \int_0^{\pi/2} |F(q;H,R,\phi)|^2 P(\phi)\sin(\phi)d\phi, \tag{3}$$

where $P(\phi)$ is the orientational distribution function. If the disks are randomly oriented, $P(\phi) = 1$, and the form factor decreases as q^{-2} at large q [27]. In Fig. 2 we show a comparison of the measured SAXS pattern $I_s(q)$ with the form factor $\overline{F^2}(q;R,H)$. Here we assumed $P(\phi) = 1$ because $I_s(q)$ roughly follows a q^{-2} power-law decay. From this comparison we estimate $R = 12.5 \pm 0.25$ nm and $2H = 1.0 \pm 0.1$ nm. These numbers are in good agreement with the values reported previously [6–10]. The results confirm that the diluted suspension is a dispersion of randomly oriented colloidal disks. The same results are obtained in the gel phase at higher volume fraction. The gel is therefore also a collection of randomly oriented colloidal disks.

Surprisingly, previous papers have not considered the polydispersity of the particle sizes, whereas this is usually an important consideration when dealing with colloids [1,28,29]. The crystal structure of the colloidal disk in the direction normal to the face is well known [5]. It is comparable to mica and other montmorillonites. Therefore the colloidal disks have a well-defined thickness of $2H = 1.0$ nm without variance. This was checked by wide-angle x-ray scattering measurements. The disk radius, however, is deter-
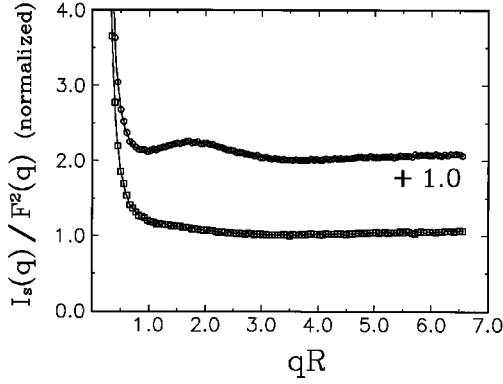
FIG. 3. Structure factors of a sol (circles) and a gel (squares) in the intermediate regime in qR. The SAXS patterns have been divided by the polydisperse form factor, and scaled to unity at the minimum. The upper curve has been shifted for clarity. The sol shows a peak that corresponds to nearest-neighbor correlations, which is absent in the gel. Both curves show a strongly increased structure factor at small qR.

mined by the complicated process of synthesis of the mineral mix and the raw mechanical process of milling [5]. We have calculated the effect of polydispersity in the radius by convoluting Eq. (3) with a normalized Gaussian distribution,

$$\Psi(R) = (\Delta\sqrt{\pi})^{-1}\exp\{[(\mathcal{R} - \langle\mathcal{R}\rangle)/\Delta]^2\}, \qquad (4)$$

where $\mathcal{R}$ is the radius and the standard deviation Δ is the polydispersity parameter. The best fit with $\langle\mathcal{R}\rangle = R = 12.5 \pm 0.25$ nm and $\Delta = 4 \pm 1$ nm, as shown in Fig. 2, agrees much better with the experimental data than the previous monodisperse models. Estimates of the error in the average radius R and the polydispersity Δ can be made separately. The model of the form factor [Eq. (3)] is very sensitive to the average radius R, especially at large q values, hence the precise value of R. The polydispersity parameter Δ has only a moderate influence, mainly at small q values. Therefore Δ is less accurately constrained

In the remainder of this paper we translate the scattering vector q to an effective scattering vector qR in order to compare the average disk diameter R with the length scale of scattering, $2\pi/q$. In the next section we will study the static structure factor of the colloidal disk arrangement on the large length scales.

B. Structure factor of colloidal arrangement

The structure factor $S(q)$ is depicted in Fig. 3. It is obtained from Eq. (1) by dividing the measured intensity pattern $I_s(q)$ by the polydisperse form factor $\overline{F^2}(q)$. In Fig. 3 we take a closer look at the intermediate regime in qR. The upper curve was measured on the fluid-like sol right after sample preparation. A peak around $qR = 2.0$ is visible, suggesting an average interparticle distance of $2\pi/q = 39$ nm. This length scale agrees very well with an effective interparticle distance, $a_{\text{eff}} = (1/\rho)^{1/3} = 34$ nm, for a random structure. Here, $\rho = 2.45 \times 10^{22}$ m^{-3} is the number density of colloidal particles corresponding to the volume fraction $\Phi_v = 0.0119$. Thus the structure factor of the sol in the intermediate regime
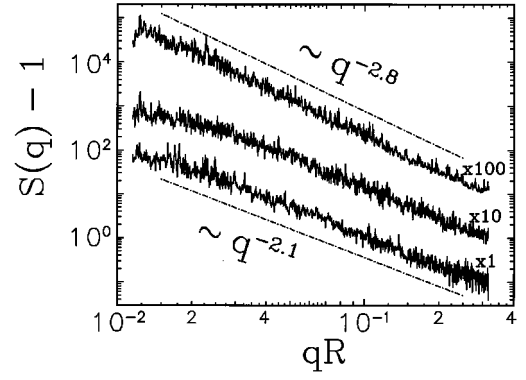

FIG. 4. Time series of the static structure factor $S(q) - 1$ vs qR as measured on the colloidal suspension of disks with a volume fraction $\Phi_v = 0.0119$ in water. At this volume fraction a strong gel is formed in 100 h. The patterns are plotted in the following order (from top to bottom); $T = 2.5$ h, 98 h, and 1.5 years. The patterns show an algebraic dependence, characterized by an exponent d that decays from $d = 2.8$ at $T = 2.5$ h to $d = 2.1$ at $T = 1.5$ years.

is similar to the structure factor of a low-density hard-sphere liquid. The lower curve was measured on the solidlike gel in which no significant time-dependent changes were observed anymore. Clearly no such particle correlations exist in the gel.

With the static light scattering (SLS) setup we can probe $S(q)$ in the regime $qR = 10^{-2} - 3 \times 10^{-1}$. Here $I_s(q)$ is proportional to the structure factor $S(q)$ because the form factor $F(q) = 1$. Thus we obtain the same quantity as depicted in Fig. 3, namely, $S(q)$, but on a different regime in qR. The results are shown in Fig. 4 at different stages of the transition from a fluidlike sol to a solidlike gel. Here we have studied the suspension of colloidal disks in water with a volume fraction $\Phi_v = 0.0119$, which forms a gel in 100 h [12]. $I_s(q)$ shows a pronounced algebraic decay with qR at the larger qR values. This is typical for a structure with self-similar, or fractal, properties [30]. In general this description applies only in an intermediate range for which both inequalities $qR \ll 1$ and $q\xi \gg 1$ are fulfilled. Here ξ is a correlation length, which can in principle be infinite but which is in practice limited by the sample container dimensions. For a self-similar object one finds [31]

$$S(q) - 1 = Aq^{-d}, \qquad (5)$$

where A is a constant and d the algebraic exponent. Equation (5) predicts that with increasing q the $S(q)$ decays towards a plateau value, which is shown in Fig. 1. The measured $I_s(q)$ curves started roughly at the same plateau value A. Therefore we have normalized $I_s(q)$ to A and subtracted unity. Matching Eq. (5) to the resulting patterns reveals the existence of a power-law decay in $I_s(q)$ over the experimental qR range accessible by SLS, as shown in Fig. 4. At $T = 2.5$ h the algebraic exponent $d = 2.8$. Then, as the system evolves we see after 12 h that the algebraic exponent has decreased to $d = 2.2$. In later stages the signal $I_s(q)$ hardly changes and the algebraic exponent seems to converge to a value of 2.1. Measurements on a year old gel, where the algebraic exponent indeed equals 2.1, support this finding.

In this section we have seen that the large length scale structure of the sol is observed to be similar in the solidlike gel. Therefore the sol is not comparable to a simple liquid but can be considered a low-viscosity precursor of the solid gel.

C. Time-dependent processes

The viscosity of the colloidal gels can be tremendously reduced by shear forces. Shear measurements by Willenbacher [14] reveal the possibility of preparing a low-viscosity initial state of the laponite suspension in a reproducible manner. Phenomenologically it is then observed that the immobile arrangement of colloidal disks, macroscopically observed as the gel, is always restored. The question is now how this final state is reached, and whether or not this is the stable state of the suspension. Therefore we have performed SAXS measurements while this ''restoring'' process was taking place. Instead of preparing samples in a large container and applying random shear (i.e., stirring), we inserted the colloidal suspensions with great force in between the narrowly spaced container windows (aspect ratio >100). We have observed the presence of relaxation processes after application of the resulting shear forces to the suspensions, on which we will report in the next two sections.

1. Large qR regime, form factor

In Fig. 5 we show a typical SAXS pattern series obtained at the Daresbury SRS for the colloidal disk suspension in a kapton windowed container. In this figure we have rescaled the vertical axis with $(qR)^2$, because $F(q)$ of randomly oriented disks decays as q^{-2}. In such a plot any deviation from this behavior is readily seen. Initially, we observe that $(qR)^2 F(q)$ is a constant. The starting situation is indeed a system of randomly oriented disk, as expected for a sol. Within a few hours, however, the form factor decreases faster than $(qR)^2$. This suggests that the disks are preferentially oriented with their faces perpendicular to the x-ray beam (see below). After 8 h this process is reversed, and after 40 h an almost constant signal is measured, indicating that the final gel state also has a random orientation of the disks. The whole process occurred on the same time scale regardless of whether the suspension was inserted into the sample container as a fluidlike sol or as a solidlike gel. Thus, after the application of shear the system has lost all memory of its previous history. In addition, we find no pronounced differences when using kapton or mica as window materials, although these materials are quite different. Mica closely resembles the chemical composition of the clay particles, whereas kapton quickly acquires a static electric charge when handled.

We interpret our data in terms of a preferential disk orientation due to flow of the suspension under shear forces. The integration of Eq. (3) is performed by incorporating a well-defined orientational distribution function $P(\phi)$ [3]. Nematic ordering is characterized by the nematic order parameter S_2 according to

$$P(\phi) = 1 + \tfrac{5}{4} S_2 [3 \cos^2(\phi) - 1]. \qquad (6)$$

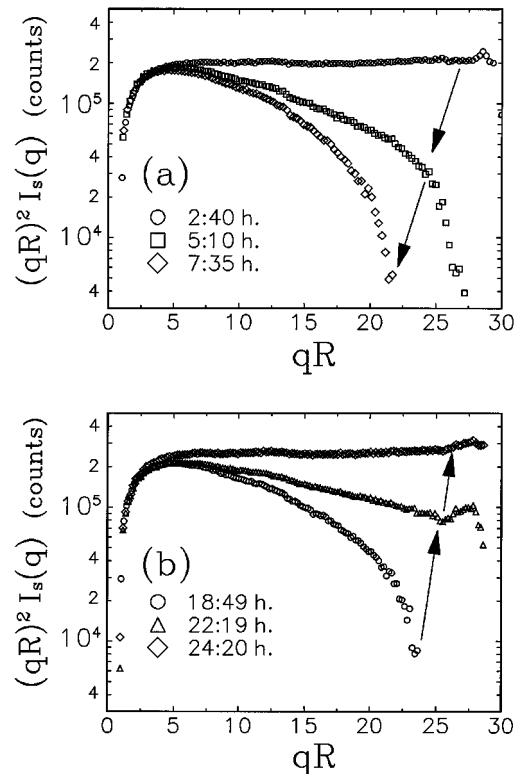We will limit the study to the nematic part because $I_s(q)$

FIG. 5. Typical series of SAXS patterns of the colloidal suspension of disks as obtained at the Daresbury SRS. The suspension was inserted into the sample container from the sol state. In the legend the time after preparation is related to the symbols. The original SAXS patterns have been multiplied with $(qR)^2$. First the pattern tends to decrease at the larger qR values, as shown in (a). After 10 h this process is reversed and the original signal is obtained after 40 h, as shown in (b). The tendency observed here is independent of the initial state before shear (sol or gel).

measured with the one-dimensional detector at Daresbury cannot give reliable information on the higher order orientational terms. In Fig. 6 we show the time dependence of the nematic order parameter S_2, obtained by comparing the results of the integration with the results as shown in Fig. 5. First S_2 tends to increase. This indicates a preferential ordering of the colloidal disks parallel to q, i.e., orthogonal to the incident x-ray beam. As time proceeds the order parameter decreases and reaches zero again, i.e., the isotropic distribution is restored. The error bars on S_2 in Fig. 6 are mainly determined by background corrections, which become increasingly important at the large qR.

2. Intermediate qR regime, structure factor

The SAXS patterns obtained at the ESRF are recorded with a two-dimensional detector. Here we obtain information not only as a function of the scattering vector q but also as a function of the azimuthal angle α. The azimuthal angle α is defined as the angle between the scattering plane and a reference plane, which we take to contain the y axis in the detection plane. Thus one has the opportunity to investigate the presence of ordering effects, both positional and orientational, in the colloidal structure [32]. Orientational ordering will be reflected as an anisotropy in the intensity pattern in
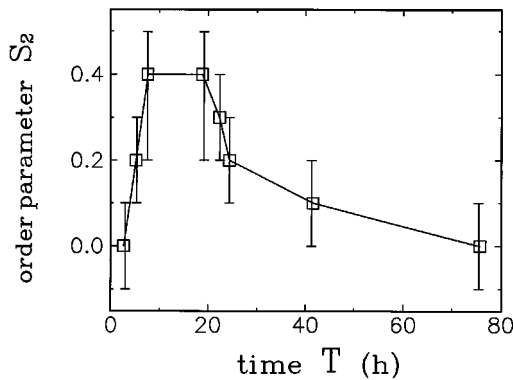
FIG. 6. Time dependence of the nematic order parameter S_2 characterizing the distribution function of the disk orientation, fitted to the data of Fig. 5. The positive value of S_2 indicates a preferential ordering of the colloidal disks as facing the container walls. The error bars on S_2 are mainly determined by background corrections, which become increasingly important at the large qR.

the two-dimensional plane of detection, depending on the angle between the director and the scattering vector.

In Fig. 7 we show the scattered intensity pattern right after injection of the colloidal suspension into the sample
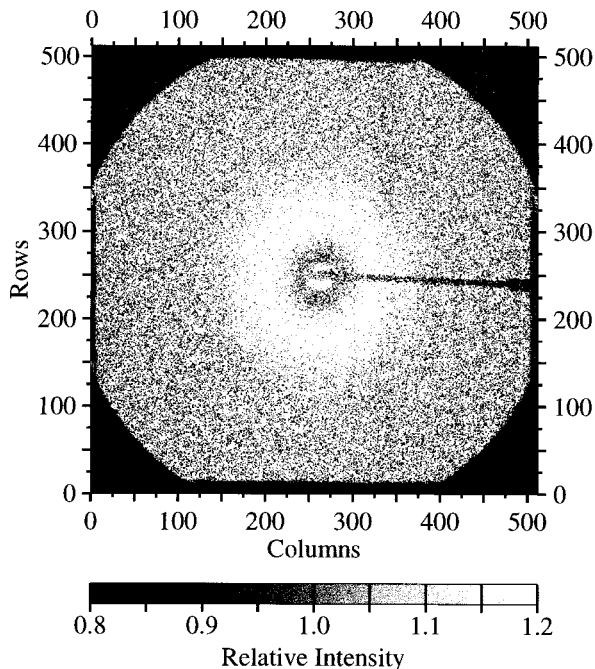

FIG. 7. The two-dimensional SAXS pattern right after inserting the gel-state suspension into the sample container ($T = 0.5$ h) divided by the scattering pattern measured at late times ($T = 50$ h). On the horizontal and vertical axis the number of the detector channel is depicted. The shadow of the beam stop is seen as the black stripe from the right to the center of the plot. A prominent feature is the presence of a ring, caused by nearest-neighbor correlations. The ring and other features are observed to have an almost perfect rotational symmetry and are independent of the sample orientation with respect to the incident x-ray beam.

container. In order to analyze the variations in detail, we have divided all two-dimensional patterns by the last pattern, recorded after a few days [33] when no changes were observed over periods of hours. This last intensity distribution is independent of α. It exactly fits the form factor measured on the dilute sample discussed above, except for the region of $qR < 5 \times 10^{-2}$ where the intensity increases with a power law as observed in the light scattering data. The prominent feature in Fig. 7 is the presence of a ring, corresponding to the average interparticle separation (cf. Fig. 3). Integrating these two-dimensional patterns over the azimuthal angle α yields the familiar one-dimensional structure factor as shown in Fig. 8. The result has a form that one would expect for a low density liquid or dense gas. As time progresses the first peak shifts to somewhat higher values, broadens, and eventually disappears. The variance in the average nearest-neighbor distance increases until the distribution merges with the low-wave-vector distribution.

At first sight the two-dimensional pattern in Fig. 7 looks independent of α. However, a plot of the intensity on the ring as a function of azimuthal angle α reveals a slight sinusoidal variation. In Fig. 9 we show the scattering intensity $I_s(q, \alpha)$ on the ring at several moments in time after sample preparation, as a function of the azimuthal angle α. Again the patterns have been divided by the pattern measured after a few days. The small variation in $I_s(q, \alpha)$ gradually decays in time. The signal-to-noise ratio is such that a quantitative determination of an order parameter cannot be reliably made. The observed sinusoidal variation is independent of sample orientation with respect to the incident x-ray beam, and the state of the suspension before insertion.

For an assessment of the amount of orientational order from the variations shown in Fig. 9, we have performed experiments on a completely orientationally ordered sample.
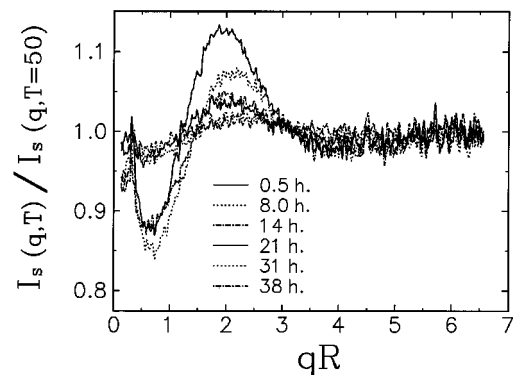

FIG. 8. Typical series of the integrated (one-dimensional) SAXS scattered intensity pattern after dividing the recorded patterns by the constant signal at $T = 50$ h. Specifically at the region of the plateau of Fig. 2, which hardly shows any structure at first sight, the relative signal shows significant changes in the first few hours after inserting the suspension. This behavior slows down considerably towards $T = 50$ h. The peak at $qR = 2.0$ corresponds to the ring as shown in the two-dimensional patterns of Fig. 7. Note the drastic decrease in depth of the crest at $qR = 0.5$ between $T = 14$ h and $T = 21$ h. Again the observations under different orientation of the sample container result in identical results.

This sample was prepared by slowly drying a gel sample, contained in a long cylindrical stock tube, until a hard transparent dime of a few millimeter thickness formed. In Fig. 10 we plot the scattering intensity $I_s(q,\alpha)$ as a function of the azimuthal angle α when the dime was placed at various angles between the normal and the incoming beam. The figures correspond to a perfectly aligned smectic system of disks with long-range orientational order [3,34]. The desicated sample consists of stacked layers of colloidal disks. In these layers the colloidal disks are translationally disordered with their surface normal directed perpendicular to the layer sequence. Comparing the results of the ordered desiccated sample with the gelating suspension in Fig. 7 and Fig. 9, it is obvious that the gelating suspension shows only a weak liquid-crystalline short-range order. In this section we have seen that at intermediate qR there are weak effects present, indicating that no collective ordering is present. At large qR we have seen strong effects (see previous section), indicating that single disks are indeed oriented. Taking these considerations into account we do not believe that the system has entered a liquid crystalline state or that the isotropic-nematic phase transition has taken place.

IV. DISCUSSION

In this paper we have presented static scattering experiments on the transition from a fluidlike sol to a solidlike gel of a suspension of disk-shaped charged colloidal particles. By employing a combination of light scattering and small angle x-ray scattering, the measurements extend from subparticle length scales to length scales of more than 250 times the average particle diameter. The starting point of the gelation is a fluidlike (low viscosity) ''sol'' of individually dispersed colloidal disks. This state can be prepared by the application of high amplitude shear onto the colloidal suspension. In practice this is done either by vigorous stirring the suspension when mixing the colloidal powder with demineralized water or by injecting a suspension with a high flow rate in between a narrow gap. It takes 5–10 h to reach a homogeneous low-viscosity state [12] consisting of single colloidal particles. The gelation then proceeds at constant density and temperature. No phase separation is observed to occur, i.e., no dense solidified gel below a dilute gaseous suspension of colloidal disks.

The structure factor has been measured for a suspension at a volume fraction $\Phi_v = 0.0119$, which has a gelation time of 100 h. In the regime $qR < 0.5$, a characteristic algebraic wave-vector dependence of the structure factor is measured right from the start of the entire gelation process. In time the algebraic exponent changes continuously from 2.8 to 2.1. The value of 2.1 in the final gel state corresponds to the value for the fractal dimension d_f of gels of spherical particles and polymers formed via an aggregation process [35–37]. In these systems the fractal dimension of 2.1 is considered to be the dimension of a structure formed by a diffusion (or chemically) limited aggregation process, where clusters with a characteristic density grow as a function of time. In contrast to these systems the gelation studied here is not an aggregation process. There is not a preferred length scale observed at any time during the gelation process. We do not observe a maximum in the structure factor, which might point to a characteristic size of a cluster that grows as the gelation proceeds. Neither do we observe a low-wave-vector cutoff that defines a correlation length. If there is a correlation length it must be longer than the maximum length of 6000 nm as probed by our light scattering measurements. This length corresponds to 170 times the average interparticle distance or 240 times the average radius of the disk. At first sight this result contradicts the results of a similar study by Pignon *et al.* [11], who have observed a characteristic correlation length in a gel of colloidal disks. However, Pignon *et al.* studied samples with volume fractions so high that the gelation times are of the order of the time necessary to disperse the disks. When the gelation and dispersion processes overlap in time, undissolved stacks of colloidal disks may be present, giving rise to the observed correlation length.
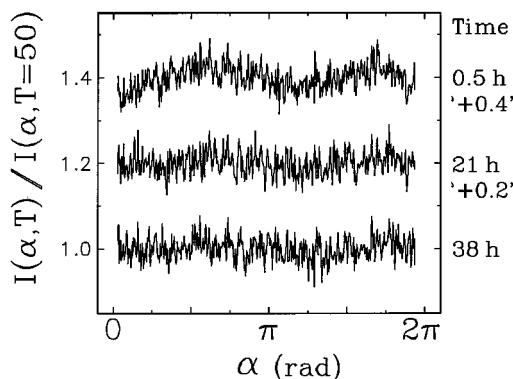

FIG. 9. The scattering intensity $I_s(q,\alpha)$ as a function of the azimuthal angle α of the data as shown in Fig. 7. The data have been averaged over a range in $qR \in [1.56, 2.19]$ centered around the maximum position in qR of the ring. The patterns shown reflect the behavior of $I_s(q,\alpha)$ at the location of the ring-shaped feature as seen in Fig. 7. In time the angular variations are observed to gradually decay.
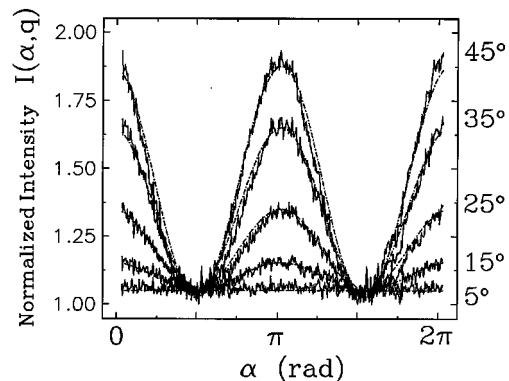

FIG. 10. The scattering intensity $I_s(q,\alpha)$ as a function of the azimuthal angle α recorded on the dried gel. The data have been averaged over a range in $q \in [1.56, 2.19]$ centered around the position of the peak observed in Fig. 8. The curves can be perfectly matched to a simple cosine function with an amplitude increasing almost linearly with the angle of orientation of the fragment.

The static structure encountered in the final gel state with a characteristic algebraic exponent of 2.1 corresponds rather to the class of fractal materials described by Maynard [38]. Like aerogels [39], the materials are founded on hierarchical structures, in contrast to percolating networks or aggregates with filaments and dangling bonds (occupied sites that do not contribute to the structure and rigidity of the network). Following the arguments of Maynard [38] and Courtens [39] we have calculated the spectral dimension γ of the spectral density $S(\omega) \propto \omega^{-\gamma}$ for a structure of plates with a fractal dimension $d_f = 2.1$ without any dangling bonds. An additional exponent σ is required, which relates the elasticity of the network to the density and is set to unity [38,39]. The resulting value of $\gamma = 1.0$ is close to the value of $\gamma = 0.86$ observed by dynamic light scattering on the laponite system [12,13]. A lower value for γ can possibly be explained by assuming a certain amount of dangling bonds and consequently a less rigid structure. Thus we find for the gel phase a close correspondence of the dynamic and static scaling behavior with the propositions of Ref. [38] and Ref. [39]. We may extrapolate this description to the low-viscosity sol phase. There we have found a spectral exponent $\gamma = 0$ from wavelet analysis [13]. This is consistent with even less rigidity. In the picture sketched here we have monitored the transformation of a structure that has many dangling bonds and no rigidity at all into a structure with a low amount of dangling bonds and a high rigidity.

Since the gelation is not an aggregation process, which involves changes in the positional correlations, one may still wonder if aggregation of orientationally correlated clusters accompanies the gelation process. Measurement of the form factor after applying shear to the suspensions reveals an initially random orientation of the disks. Within a few hours, however, an orientational ordering of the disks is observed. After reaching a maximum in the order parameter S_2, the suspensions reveal a restoring of the random orientation of the colloidal disks until the highly viscous, elastic gel state is reached. At first sight it seems surprising that the colloidal disks tend to order orientationally before returning to a state with random orientations. However, when squeezing a gel in between two plates, Pignon *et al.* have observed thin low-viscosity boundary layers where the bulk of the gel is sliding through [40]. In our case, a thin low-viscosity boundary layer with presumably high liquid crystalline order exists close to the walls of the sample cell, surrounding an elastic gel in the middle. The observed growth of nematic order is induced from the boundary layer inwards, becoming thicker as time progresses. At the same time, local reorientation driven by thermal motion breaks down the order, overtaking the first process and eventually leading to the observed random gel state. This explains the behavior of the order parameter S_2 as a function of time.

Nowhere along the path to gelation, however, is there a long-range orientational correlation. If there is a correlation length associated with the orientational order it only extends to the nearest neighbors and becomes shorter as the measurements of the structure factor in Fig. 8 and Fig. 9 indicate. In Fig. 8 we observe a structure factor one would expect for a normal liquid. The first peak at $qR = 2.0$ corresponds to an interparticle separation of 39 nm, substantially larger than

the average diameter of the disks of 25 nm. One would expect this structure factor for a random stacking of spheres with a diameter of 34 nm. The volume of this sphere is roughly equal to the volume cut out by the colloidal disk taking into account an estimate of the Debye screening length of an orientationally averaged screened Coulomb potential [41]. In this regime of qR we look at mutual orientation ordering. The measurements reveal that the T-shaped configuration, the favored unit in the suggested ''house of cards'' structure for the gel, is absent. It would show up in the structure factor at shorter length scales [23]. Dijkstra *et al.* [23] showed that the quadrupolar character of the screened Coulomb potential is essential in the formation of the gel phase. In their Monte Carlo study they used a system of infinitely thin disks with a point quadrupole moment. The model carries the essential features of the interparticle interaction of the real colloidal disk system. Without the quadrupolar interaction the system exhibits the isotropic to nematic phase transition according to the Onsager criterion [4]. With the quadrupolar interaction turned on they show that the system undergoes a transition from a low density phase, where the disks assemble into ''elongated chainlike clusters,'' to a rigid gel phase at higher densities. The gel exhibits a nearly incompressible network structure similar to the ''house of cards'' structure thought to be typical of clay gels. At these high densities the quadrupolar interaction favors edge-to-face pair configurations (T-shaped units) that counteracts the parallel alignment of bare hard disks.

In the real colloidal disk system gel formation occurs at lower volume fractions. At these lower volume fractions we find no evidence for an on-average T-shaped configuration to form the house of cards structure in the gel phase. The measurements indicate that the formation and growth of orientational clusters is not the road towards gelation. There is no orientational order left in the gel phase. The results do suggest that local reorientations are essential in the transformation of the fractal structure. We have experimentally monitored a dynamic process where a fractal structure with many dangling bonds and low elasticity transforms into a fractal structure with a low amount of dangling bonds and a high rigidity. This transition is made possible by continuous local reorientation of the colloidal disks, which allows more and more particles to become part of the network. In time the rigidity and elasticity of the colloidal structure increases, the viscosity diverges, and the solid phase is formed in close analogy with the glass transition.

[1] P. N. Pusey, in *Liquids, Freezing and Glass Transition*, edited by J. P. Hansen, D. Levesque, and J. Zinn Justin (North-Holland, Amsterdam, 1991), p. 765.

[2] L. Onsager, Ann. (N.Y.) Acad. Sci. **51**, 627 (1949).

[3] P. G. de Gennes and J. Prost, *The Physics of Liquid Crystals* (Clarendon, Oxford, 1993), 2nd ed.

[4] D. Frenkel, in *Liquids, Freezing and Glass Transition*, edited by J. P. Hansen, D. Levesque, and J. Zinn Justin (North-Holland, Amsterdam, 1991), p. 689. See also J. A. C. Veerman and D. Frenkel, Phys. Rev. A **45**, 5632 (1992).

[5] Laponite (RD) is manufactured by Laporte Absorbents, P.O. Box 2, Cheshire, UK.

[6] J. D. F. Ramsey, J. Colloid Interface Sci. **109**, 441 (1986).

[7] R. G. Avery and J. D. F. Ramsey, J. Colloid Interface Sci. **109**, 448 (1986).

[8] L. Rosta and H. R. von Gunten, J. Colloid Interface Sci. **134**, 397 (1990).

[9] D. W. Thompson and J. T. Butterworth, J. Colloid Interface Sci. **151**, 236 (1992).

[10] A. Mourchid, A. Delville, and P. Levitz, Faraday Discuss. **101**, 275 (1995).

[11] F. Pignon, J. M. Piau, and A. Magnin, Phys. Rev. Lett. **76**, 4857 (1996). See also F. Pignon, A. Magnin, J. M. Piau, B. Cabane, P. Lindner, and O. Diat, Phys. Rev. E **56**, 3281 (1997).

[12] M. Kroon, G. H. Wegdam, and R. Sprik, Phys. Rev. E **54**, 6541 (1996).

[13] M. Kroon, G. H. Wegdam, and R. Sprik, Europhys. Lett. **35**, 621 (1996).

[14] N. Willenbacher, J. Colloid Interface Sci. **182**, 501 (1996).

[15] W. Götze and L. Sjögren, Phys. Rev. A **43**, 5442 (1991).

[16] J. P. Sethna, Europhys. Lett. **6**, 529 (1988).

[17] D. Kivelson, S. A. Kivelson, X. Zhao, Z. Nussinov, and G. Tarjus, Physica A **219**, 27 (1995).

[18] E. Bartsch, M. Antonietti, W. Schupp, and H. Sillescu, J. Chem. Phys. **97**, 3950 (1992).

[19] W. van Megen, S. M. Underwood, and P. N. Pusey, Phys. Rev. Lett. **67**, 1586 (1991).

[20] G. Li, W. M. Du, J. Hernandez, and H. Z. Cummins, Phys. Rev. E **48**, 1192 (1993).

[21] See, e.g., C. A. Herbst, R. K. Cook, and H. E. King, Nature (London) **361**, 518 (1993); M. J. P. Brugmans and W. L. Vos, J. Chem. Phys. **103**, 2661 (1995).

[22] H. van Olphen, *Clay Colloid Chemistry*, 2nd ed. (John Wiley, New York, 1977).

[23] M. Dijkstra, J. P. Hansen, and P. A. Madden, Phys. Rev. Lett. **75**, 2236 (1995); Phys. Rev. E **55**, 3044 (1997).

[24] P. Bösecke, O. Diat, and B. Rasmussen, Rev. Sci. Instrum. **66**, 1636 (1995); P. Bösecke and O. Diat (unpublished).

[25] W. Bras *et al.*, J. Phys. IV (France) **3**, 447 (1993).

[26] A. Guinier and G. Fournet, *Small Angle Scattering of X-rays* (Wiley, New York, 1955).

[27] In the limit $H \to 0$ the first factor on the rhs of Eq. (2) becomes equal to unity. In the limit of large q, Eq. (3) can be rewritten as an integral over the decaying Bessel function squared. This gives a constant divided by the remaining factor q^2.

[28] H. G. Barth and S. T. Sun, Anal. Chem. **65**, 55R (1993).

[29] M. Megens, C. M. van Kats, P. Bösecke, and W. L. Vos, Langmuir **13**, 6120 (1997).

[30] *On Growth and Form, Fractal and Non-Fractal Patterns in Physics*, edited by H. E. Stanley and N. Ostrowsky (Kluwer, Dordrecht, 1986).

[31] J. Teixera, in *On Growth and Form, Fractal and Non-Fractal Patterns in Physics* (Ref. [30]), p. 145.

[32] W. L. Vos, M. Megens, C. M. van Kats, and P. Bösecke, Langmuir **13**, 6004 (1997).

[33] We have divided all two-dimensional patterns by the last pattern recorded ($T = 50$ h), because (i) $I_s(q)$ spans almost three orders of magnitude, which obscures small variations, (ii) uncertainties in the background level and local detector overload introduce additional inaccuracies when dividing $I_s(q)$ by the form factor, (iii) a few days is well beyond the restoring time of the gel, thus the figure shows the relative deviation from the constant (relaxed) signal.

[34] A. J. Leadbetter, in *The Molecular Physics of Liquid Crystals*, edited by G. R. Luckhurst and G. W. Gray (Academic Press, New York, 1979), p. 296.

[35] M. Kolb, R. Botet, and R. Jullien, Phys. Rev. Lett. **51**, 1123 (1983).

[36] D. W. Schaeffer and K. D.Keefer, in *Fractals in Physics*, edited by L. Pietronero and E. Tosatti (Elsevier, Amsterdam, 1986), p. 39.

[37] P. W. Rouw and C. G. de Kruif, Phys. Rev. A **39**, 5399 (1989).

[38] R. Maynard, Physica A **157**, 601 (1989); G. Deutscher, R. Maynard, and O. Parodi, Europhys. Lett. **6**, 49 (1988).

[39] E. Courtens, J. Pelous, J. Phalippou, R. Vacher, and T. Woignier, Phys. Rev. Lett. **58**, 128 (1987); E. Courtens, in *Fractals in Physics*, edited by A. Aharony and J. Feder (North-Holland, Amsterdam, 1989).

[40] F. Pignon, A. Magnin, and J. M. Piau, J. Rheol. **40**, 573 (1996).

[41] E. Trizac and J. P. Hansen, J. Phys. Condens. Matter **8**, 9191 (1996).